Contrib Mineral Petrol (1984) 86:209–220

Contributions to Mineralogy and Petrology

Petrogenesis of calc-alkaline, shoshonitic and associated ultrapotassic Oligocene volcanic rocks from the Northwestern Alps, Italy

G. Venturelli[1], R.S. Thorpe[2], G.V. Dal Piaz[3], A. Del Moro[4], and P.J. Potts[2]

[1] Istituto di Mineralogia, Universita di Parma, Parma, Italy
[2] Department of Earth Sciences, The Open University, Milton Keynes, UK
[3] Istituto di Geologia, Universita di Padova, Padova, Italy
[4] Istituto di Geocronologia e Geochimica Isotopica CNR, Pisa, Italy

Abstract. Along the Western Alps there is geological evidence of late-Alpine (Oligocene) magmatic activity which clearly postdates the Lepontine (Eocene-early Oligocene) metamorphism and related deformation of the Alpine nappe pile. This magmatic activity was notably delayed in relation to the most important convergent processes and may be related to buoyancy of lithosphere, tensional tectonics and thermal updoming subsequent to the collision between the Eurasian and African plates. The geochemical features of the rocks and the geophysical characteristics of the Alpine chain, suggest that: (a) shoshonitic and calc-alkaline melts may have been generated by partial melting of metasomatized peridotitic material and subsequent fractional crystallization and crustal contamination; silicic andesites and latites, however, could have been also derived from metasomatized eclogite or deep continental crust material; (b) the ultrapotassic lamprophyres with high K, P, LREE, Th, Zr, U and high $^{87}Sr/^{86}Sr$ ratios were generated by partial melting of strongly metasomatized mantle; the varied Sr-isotopic ratios may partially also reflect additional radiogenic component from the continental crust following magma segregation from the source.

Introduction

While the Tertiary plutonic bodies within the Alpine chain have been extensively investigated during this century (Boegel 1975, and references therein), the volcanic activity associated with the late evolution of the Alps has been studied in much less detail. Recently, however, it has become apparent that late-Alpine volcanic rocks and dykes are widespread along the whole Alpine chain from the Aosta valley (Fig. 1) to the Austria-Jugoslavia Alps. This magmatic activity postdates the collision between the European and African plates and thus is unrelated to active subduction of oceanic crust. This paper deals with the Oligocene calcalkalic, shoshonitic and ultrapotassic activity of the Western Alps, with particular emphasis on the high-K rocks of orenditic affinity.

Geological Framework

The formation of the Alps was preceded by the opening of the Ligure-Piemontese basin (Laubscher 1969, 1974; Dal Piaz et al. 1972 and references therein). The culmination of the rifting occurred during the Jurassic, when, following fragmentation of the thinned Hercynian crust, an area of accreting oceanic crust separated the African and European plates. During the Cretaceous there was a change in the pattern of the plate motion in this sector of the Tethyan basin (Dal Piaz et al. 1972; Hunziker 1974). The European margin began to descend along a southeastward orientated subduction zone (termed the Eoalpine subduction) below the African plate. In the Western Alps the subduction involved not only the oceanic crust but also some narrow section of the disrupted European margin and of the African continental crust as independent imbricated sheets. During the Eoalpine compressional stage both the oceanic and continental crust experienced high P-low T metamorphism and related deformation. Mineral assemblages ranging from eclogite to blueschist facies are locally well preserved in the Western Alps (Dal Piaz et al. 1972; Bocquet et al. 1974; Frey et al. 1974; Dal Piaz and Ernst 1978, and references therein).

There is no direct evidence of Eoalpine magmatic activity related to this pre-collisional evolution of the convergent lithospheric plates. In the Western Alps, however, the andesitic clastics from the Tertiary Tavayanne formation (Martini 1968; Delaloye and Sawatzky 1975, with references therein) could be regarded as the possible record of this supposed andesitic magmatism.

Geochronological data on the ophiolitic eclogite and on the Austroalpine continental crust (Dal Piaz et al. 1972; Hunziker 1974; Bocquet et al. 1974; Dal Piaz et al. 1978) as well as geological evidence of very limited compressional activity during the Palaeocene suggest that the continental collision was already completed at this time. During the late Eocene-early Oligocene the progressive uprise of the isotherms generated the greenschist to amphibolite facies regional metamorphism (Lepontine event, about 38 Ma; cf. Niggli 1973; Frey et al. 1974; Hunziker 1974; Jäger 1973) as well as magmatic activity.

From the Oligocene the Alpine pile of nappes experienced rapid uplift of its axial sector (Wagner et al. 1977) and strong erosion with molasse deposition. At this time, intrusions (Biella, Traversella and Miagliano in the Western Alps), dykes and rare flows with calc-alkaline to ultrapotassic characteristics were emplaced in the investigated area close to the Canavese tectonic line (Fig. 1). The rocks of the investigated area yield isotopic ages in the range 29–33 Ma (Krummenacher and Evernden 1962; Carraro

Offprint requests to: G. Venturelli

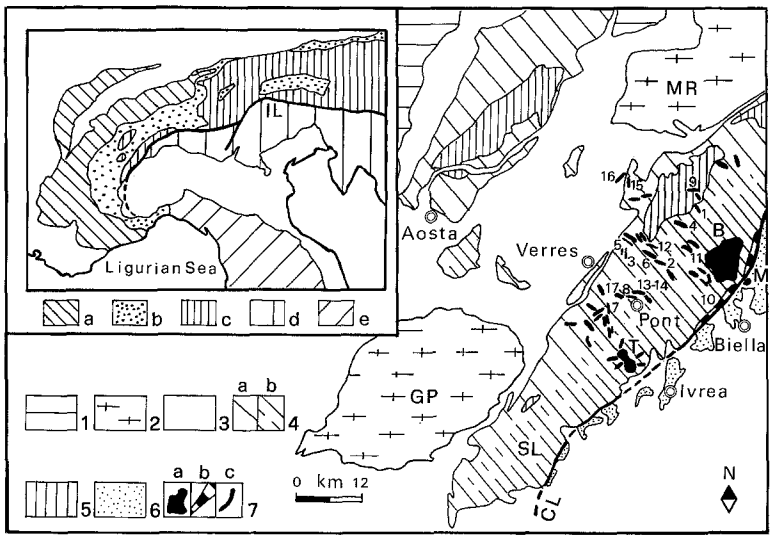

Fig. 1. Geological sketch map of the Internal Northwestern Alps *Tectonic Units:* 1) Gran San Bernardo Nappe; 2) Pennine Monte Rosa (*MR*), Aresa-Brusson and Gran Paradiso (*GP*) nappes; 3) Undifferentiated Piemonte ophiolite nappe and Roisan Zone; 4) Austroalpine tectonic system: Sesia-Lanzo Unit (*SL*) and Dent Blanche nappe (a-Gneiss Minuti Complex, b-Eclogitic micaschist complex; 5) Upper tectonic element of the Sesia-Lanzo and Dent Blanche nappes; 6) Undifferentiated Southern Alps including the Ivrea Zone, *CL*, Canavese tectonic line. *Igneous rocks*: 7(a) Oligocene stocks of Biella (*B*), Traversella (*T*) and Miagliano (*M*); (b) Oligocene volcanosedimentary cover of the internal Sesia-Lanzo nappe; (c) Oligocene K-rich lamprophyres and "andesitic" dykes. The locations of the analysed samples reported in Table 3 are as follows: Calc-alkaline; 1=118, 2=695, 3=1729, 4=214, 5=1710, 6=1433, 7=319, 8=251, Shoshonitic; 9=96, 10=1064, 11=241, 12=216, Ultrapotassic; 13=242, 14=243b, 15=1698, 16=1627, 17=247. The inset shows the position of the Sesia-Lanzo Unit and Dent Blanche nappe in the Alps: (a) Paleoeuropean Helvetic-Dauphinois zone and Jura; (b) Paleoeuropean Pennine zone including ophiolite units; (c) Paleoafrican Austroalpine units; (d) Southern Alps; (e) Northern Apennines. The heavy line represents the Insubric lineament

and Ferrara 1968; Dal Piaz et al. 1973; Hunziker 1974; Scheuring et al. 1974; Zingg et al. 1976).

Mineralogy and Petrography

A description of the analyzed samples is reported in Table 1 and the main features are summarized below.

Basalt-andesite-latite group

The rocks range in composition from basalt ($SiO_2 < 53$) through basaltic andesite ($SiO_2 < 56$) to andesite and latite ($SiO_2 > 56$). Many of the analyzed rocks have experienced varying degrees of deuteric transformation so that the primary phases are not always perfectly preserved. The main secondary minerals include chlorite, carbonate, epidote, albite and sericite.

The *basalts* contain abundant hornblende and plagioclase phenocrysts, and minor biotite, with apatite and Fe–Ti oxides as minor components. The *shoshonitic basalt* (sample 96) is characterized by biotite, zoned clinopyroxene and scarce amphibole phenocrysts, with a groundmass including K-feldspar, plagioclase and minor quartz. The *basaltic andesites* contain brown hornblende ± clinopyroxene ± calcic plagioclase, or biotite + clinopyroxene phenocrysts in a groundmass composed of plagioclase, quartz, and rare K-feldspar. The *andesites* are petrographically varied and range from porphyritic to aphyric in texture. When present, phenocrysts are brown hornblende and/or biotite and plagioclase, while the matrix contains plagioclase, apatite, sphene, rare K-feldspar and sometimes amphibole. The *latites* commonly have phenocrysts of biotite, zoned brown hornblende (ca. 1.2% K_2O), plagioclase and K-feldspar.

Ultrapotassic lamphrophyres

Some lamprophyres (samples 242, 243b, 247) contain abundant zoned mica, clinopyroxene and K-feldspar. Chemical data on some minerals are reported in Table 2. Clinopyroxene ranges from diopside to salite in chemical composition and is characterized by low TiO_2 (0.23–0.39%) and Al_2O_3 (0.18–1.49%), and by significant variation of the Mg/(Mg+Fe+Mn) atomic ratio (0.780–0.935). The zoned mica ranges from phlogopite to biotite in composition and is characterized by a large variation in FeO (3.1–14.9%) and TiO_2 (1.2–3.8%) content. The K-feldspar is low in Na_2O. Alkaline amphibole, Fe–Ti oxide, carbonate and rare olivine are also present. Other ultrapotassic rocks (1627, 1698) contain abundant brownviolet to green-brown alkaline amphibole (probably K-rich riebeckite-arvedsonite; De Marco 1959) and sometimes kinked crystals of mica. The groundmass consists dominantly of K-feldspar with minor clinopyroxene, apatite, sphene, and Fe–Ti oxide.

Chemical composition

Analytical methods

Chemical analyses were performed by X-ray fluorescence (Si, Al, Ti, Fe, Ca, Mn, K, P, Nb, Zr, Y), atomic absorption (Mg, Ni, Cr, Cu, V, Zn, Li), flame photometry (Na), volumetric (Fe^{2+}) and gravimetric (loss on ignition) methods (Dal Piaz et al. 1979). The Rare Earth Elements (REE), Hf, Ta, Th and U have been determined by instrumental neutron activation (INAA) following the method described by Potts et al. (1981). As estimated by comparison with international reference materials, accuracies are estimated to be in the range 5–10%. The Sr-isotope ratios were determined on a Varian MATTHS mass spectrometer, and Rb and Sr contents were determined by a standard dilution method. Measurements of the Eimer and Amend standard determined during this work yielded an overall mean of 0.70812 ± 8 (1σ). Several tests of precision on the $^{87}Sr/^{86}Sr$ ratio yielded $1\sigma = 0.0001$–0.0002 for the analyzed samples.

Results

In agreement with the petrographic features, the analysed rocks (Table 3) may be divided in three main groups: calc-

Table 1. Locations and petrographic features of the analysed samples

Calc-alkalic		
118	Becco di Cossatello, N wall, 2,330 m a.s.l. Artogna Valley	Dyke within the Sesia-Lanzo micaschists, close to the southern boundary of the 'Diorito-Kinzigitic Zone'. Porphyritic rock with abundant Amph, Pl and subordinate Bi phenocrysts. Ap and Opq also present.
695	Road within the Gressoney Valley, just below the dam of Issime	Dyke within the eclogitic micaschists of the Sesia-Lanzo zone. Abundant phenocrysts of zoned Bi and minor Cpx within a feldspathic matrix containing scarce Qz. Opq, Ap and Ca are minor components.
1729	SW wall of Becca Torché, Ayas Valley, 0.3 km N of Alpe Dondeuil, 1,950 m a.s.l.	Dyke cutting the kinzigitic micaschists of the Sesia-Lanzo Zone. Small phenocrysts of brown Amph and Pl. Granular patches of Ep which probably replaces clinopyroxene. Minor Chl, Ab, Ep, Sph in the matrix.
214	Gressoney Valley, along the road Gaby-Niel, at the bottom of the SW wall of Mt. Pianeritz	Dyke within the metagranitoids of the Sesia-Lanzo Zone. Deuterically altered porphyritic rocks with zoned Pl altered to Ep + -Ab, colourless Amph + Chl (after Ca-amph?) and Chl aggregates (after Bi?). Ru, Sph, Ilm, Ap are accessories.
1750	SW wall of Becca Torché, Ayas Valley, 0.5 km N of Alpe Dondeuil, 2,150 m a.s.l.	At the boundary between the Gneiss Minuti and the kinzigitic micaschists, Sesia-Lanzo Zone. Well preserved phenocrysts of brown-green Amph in a fine-grained matrix with with calcic-Pl and minor Qz. Opq and Ap are accessory minerals.
1433	Gressoney Valley, on the Issime – Santa Margherita road, 1,200 m a.s.l.	Abundant brown and Cpx phenocrysts. Groundmass consists of Pl, Chl and rare Qz. Ort, Ap Sph are accessory minerals.
319	Champorcher Valley, between Mt. Coco and Alpe Balma	Dyke within the Gneiss Minuti Complex, Sesia-Lanzo Zone. Well preserved phenocrysts of browngreen Amph. Fine-grained partially altered matrix including Ca–Pl, Chl, Ep, Amph, W-Mic. Opq, Sph, Ap as accessory minerals.
251	Aosta Valley, 1.3 km from Pont St. Martin, "Niou" ore deposit, 1,010 m a.s.l.	Dyke within the Eclogitic Micaschists, Sesia-Lanzo Zone. Phenocrysts of transformed Pl and brown Amph (altered to Ep, Chl, Ca). The fine-grained matrix includes Ca–Pl, Chl, rare K-Feld. Ap and Opq are minor components.
Shoshonitic		
96	Artogna Valley (Sesia Valley), Alpe Piana Bella, 2,110 m a.s.l.	Dyke cutting the Diorito-Kinzigitic Zone. Bi, zoned Cpx and subordinate Amph phenocrysts. Groundmass is composed of K-feld, Pl, minor Qz.
1064	Near Falletti, Cervo Valley (Biella), 1,100 m a.s.l. (31.5 m.y., Hunziker 1974)	Lava from the volcano-sedimentary cover of the internal Sesia-Lanzo Zone. The major minerals are: Ca–Pl, Cpx, brown Amph. Bi, Qpq, Ca are minor components. Possible K-Feld occurs in the fine-grained matrix.
241	Cervo Valley, between Piedicavallo and Issime, close to Lago della Vecchia, 2,050 m a.s.l.	Dyke within the Eclogitic Micaschists of the Sesia-Lanzo Zone. Partially altered Bi and Pl phenocrysts within a granophyric matrix containing K-Feld and scarce Pl and Qz. Ort, Opq are accessory minerals.
216	Stolen Valley (Issime, Gressoney Valley), below Alpe Muntuschuz, 1,650 m a.s.l.	Dyke within the eclogitic micaschists of the Sesia Lanzo Zone. Bi (altered to Chl, Sph, ± Ep) and Pl (to Ab, W-Mic, Chl) and zoned brown-Amph phenocrysts. Amph exhibits greens rims and is partially altered to colourless Amph, Chl, Ep, Sph. Abundant K-Feld in the groundmass. Qz, Opq, Ort, Ap are minor components.
Ultrapotassic (high-K lamprophyres)		
242, 243 b	Rio Rechantez, left side of the lower Gressoney Valley, 2.5 km NE Verres, 890 m a.s.l.	Dyke within the eclogitic micaschists of the Sesia-Lanzo Zone. Zoned and kinked B-Mic including Ol and Px, idiomorphic Cpx and large crystals of K-Feld are the main components. Altered Ol (Spt + Opq), Ap, Ort, Opq, Ca are minor components. Sample 243 b represents the inner portion of the dyke.
1698	Upper Mascognaz Valley, Champoluc, 1.2 km NE Colle Pallasina, 2,600 m a.s.l.	Dyke within the paraschists of the Sesia-Lanzo Zone close to the contact with the underlying Piemonte Ophiolite Nappe. Abundant zoned B-Mic and brown-violet alkaline Amph with K-Feld crystals in the groundmass. Ap and Sph are the minor components.
1627	Upper Mascognaz Valley, Champoluc, 0.5 km NE Colle Pallasina, 2,600 m a.s.l. (31.6 m.y., Dal Piaz et al. 1973)	Dyke cutting the calcschists of the Combin Unit (Piemonte Ophiolite Nappe). B-Mic, Amph and K-Feld in the matrix are the most abundant minerals. Cpx, Sph, Ap, Op are minor components.
247	Plan d'Albard, close to Bard (Aosta Valley), 640 m a.s.l.	Dyke within the fine-grained gneiss and micaschists of the Sesia-Lanzo Zone. Abundant flakes of zoned B-Mic with intergranular Cpx, alkaline Amp, microgranular K-Feldspar, Ap, Ca, and Opq as accessory minerals.

OL = olivine; Px = pyroxene; Cpx = Ca-pyroxene; Bi = biotite; B-Mic = biotite/phlogopite; Amph = amphibole; W-Mic = white mica; Qz = quartz; K-Feld = K-feldspar; Pl = plagioclase; Ab = albite; Ap = apatite; Ep = epidote; Sph = sphene; Chl = chlorite; Opq = opaques; Ort = orthite; Ca-carbonate; Ru = rutile; Ilm = ilmenite; Spt = serpentine

Table 2. Representative chemical analysis of some minerals from the K-rich lamprophyres from the Western Alps, Italy

	Clinopyroxene					Brown micas						K-feldspar	
	247 M	C 247 B	R	242 M	242 S	247	C 247	R 147	242	242	242	242	247
SiO_2	54.3	54.5	54.6	53.1	52.5	42.1	38.8	36.0	38.0	38.1	38.1	65.6	64.0
TiO_2	0.24	0.23	0.26	0.39	0.26	1.21	2.62	2.85	3.77	3.76	3.75	—	—
Al_2O_3	0.27	0.18	0.21	1.34	1.49	12.2	12.2	15.4	13.8	13.6	13.8	18.3	17.6
Cr_2O_3	0.06	0.15	—	—	—	0.50	0.09	—	0.60	0.12	—	—	—
FeO tot	2.59	2.34	2.92	5.46	7.22	3.01	10.7	14.9	6.48	8.68	11.2	0.20	0.96
MnO	0.10	0.11	0.17	0.22	0.30	—	0.15	0.21	0.08	0.09	0.15	0.14	—
MgO	18.5	18.9	18.2	16.2	14.4	25.6	19.1	14.3	20.1	18.8	17.2	—	—
CaO	22.9	24.0	23.3	22.5	22.2	0.05	—	—	0.07	0.07	0.05	0.08	—
Na_2O	0.14	0.13	0.17	0.23	0.30	0.11	0.12	0.25	0.29	0.30	0.32	0.56	0.26
K_2O	—	—	—	—	—	10.2	9.50	9.30	9.80	9.50	9.70	16.1	15.6
Total	99.1	100.5	99.8	99.4	98.7	95.0	93.3	93.2	93.0	93.0	94.3	101.0	98.5
Atoms													
Si	1.987	1.971	1.988	1.962	1.971	2.978	2.905	2.757	2.809	2.836	2.834	3.002	3.003
Ti	0.007	0.006	0.007	0.011	0.007	0.064	0.148	0.164	0.210	0.210	0.210	—	—
Al	0.012	0.008	0.009	0.058	0.066	1.017	1.077	1.390	1.202	1.193	1.210	0.987	0.973
Cr	0.002	0.004	—	—	—	0.028	0.005	—	0.035	0.007	—	—	—
Fe^{+++}	—	—	—	—	—	—	—	—	—	—	—	0.008	0.038
Fe^{++}	0.079	0.071	0.089	0.169	0.227	0.178	0.670	0.954	0.401	0.540	0.697	—	—
Mn	0.003	0.003	0.005	0.007	0.010	—	0.010	0.014	0.005	0.006	0.009	0.005	—
Mg	1.009	1.019	0.987	0.892	0.806	2.699	2.131	1.632	2.214	2.085	1.906	—	—
Ca	0.898	0.930	0.909	0.891	0.893	0.004	—	—	0.005	0.006	0.004	0.004	—
Na	0.010	0.009	0.012	0.016	0.022	0.015	0.017	0.037	0.042	0.043	0.046	0.050	0.024
K	—	—	—	—	—	0.921	0.907	0.909	0.924	0.902	0.920	0.940	0.934
$\frac{100 \times Mg}{(Mg+Fe+Mn)}$	92.7	93.5	91.7	84.1	78.0	93.8	76.1	63.1	84.7	79.4	73.2	—	—

B,M,S, mean large, medium and small crystal respectively. C = core, R = rim

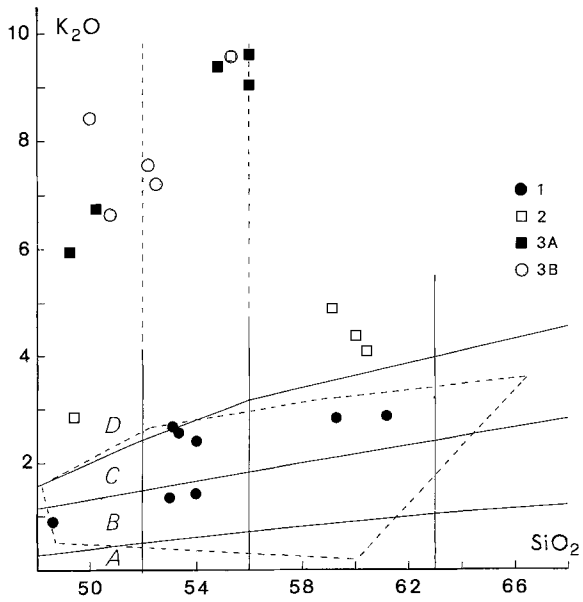

Fig. 2. Plot of K_2O against SiO_2 for the calc-alkaline (1), shoshonitic (2) and ultrapotassic (3A-this work, 3B-De Marco, 1959) rocks from the Internal Western Alps. The dashed line includes coeval volcanic/subvolcanic rocks from Eastern Alps (Beccaluva et al. 1979; Del Moro et al. 1981 and unpublished). The data have been recalculated to 100 per cent, excluding 'loss on ignition'. The labelled fields are as follows: *A*, low-K tholeiitic suite; *B*, calc-alkaline; *C*, high-K calc-alkaline; *D*, shoshonitic (cf. Peccerillo and Taylor 1976)

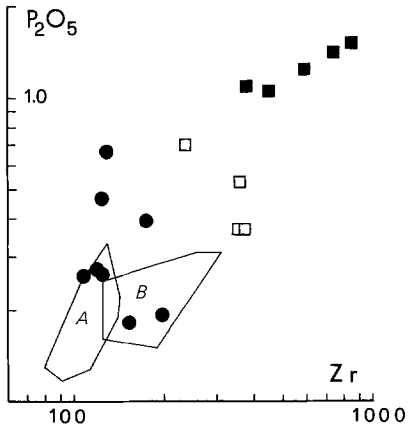

Fig. 3. Plot of P_2O_5 against Zr. Symbols as in Fig. 2. The fields of the calc-alkaline rocks from the Eastern Alps (A, Del Moro et al. 1981 and unpublished. B, Beccaluva et al. 1979) are also reported for comparison

alkaline (CG), shoshonitic (SG) and ultrapotassic (UK). The distinction between different groups is consistent with the position of the samples in the plot of K_2O against SiO_2 (Fig. 2) and P_2O_5-Zr (Fig. 3), with the Ce/Yb ratio, and with the Nb, Th, U, Rb, Hf, Ta, Zr abundances.

Calc-alkaline (CG) and shoshonitic (SG) rocks. All the rocks have Th and U contents higher than and Ce/Yb ratios similar to those of comparable rocks from active continen-

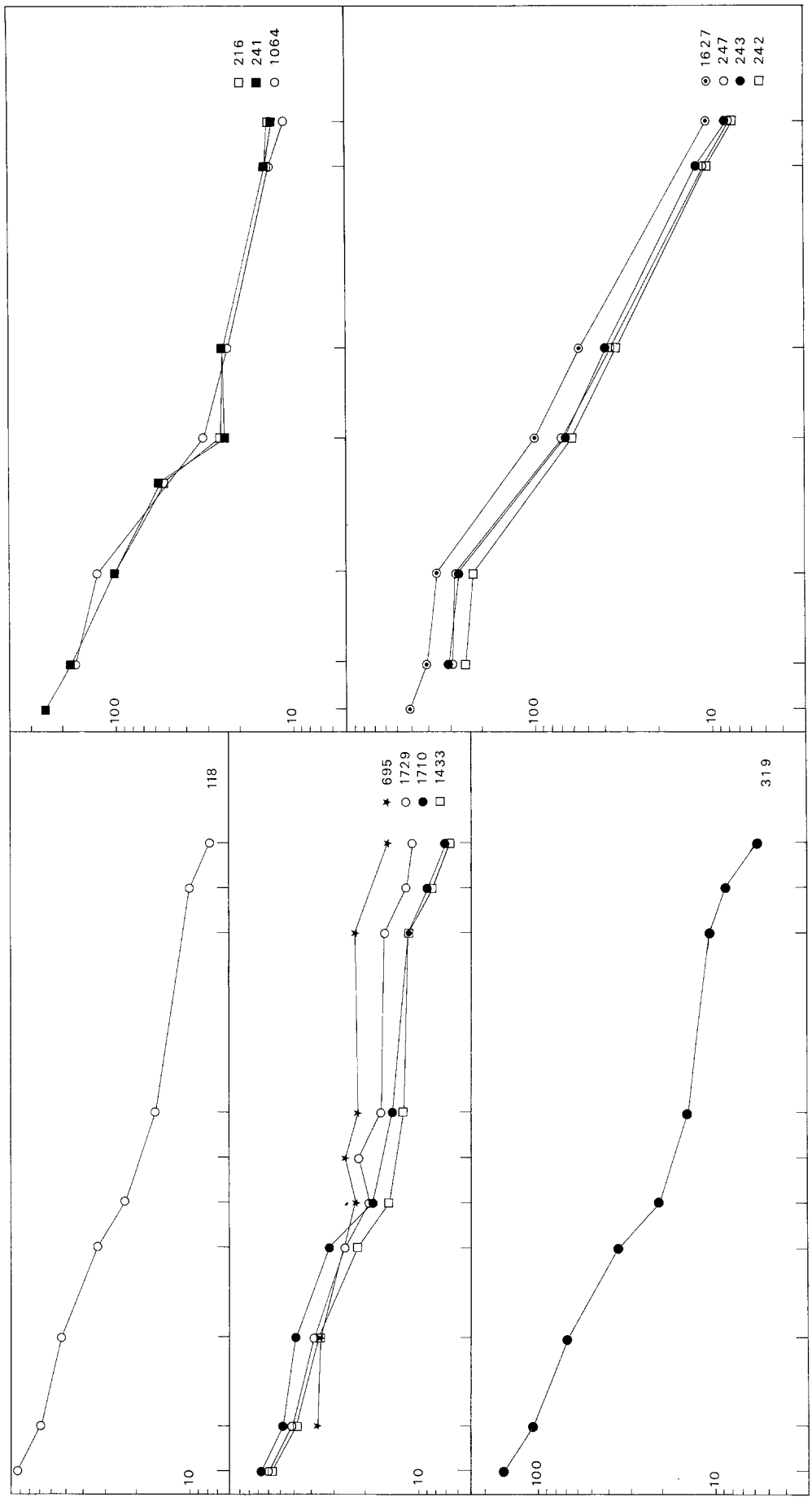

Fig. 4. Chondrite-normalized REE patterns. The normalizing values are from Nakamura (1974) with values of 0.052 and 0.034 ppm for Tb and Tm respectively

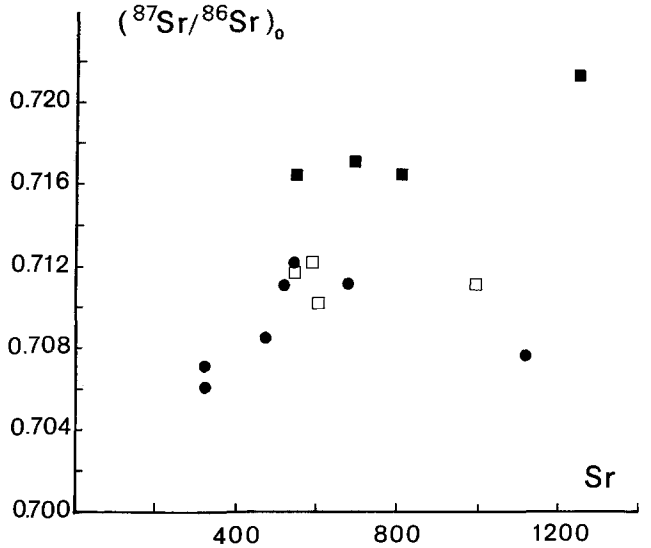

Fig. 5. Plot of initial $^{87}Sr/^{86}Sr$ ratio, $(^{87}Sr/^{86}Sr)_0$ against Sr for analysed samples

tal margins. The latites have unusually high Th and U contents which are comparable to those of the ultrapotassic rocks from the same area. Two latites have significant europium anomalies (Eu/Eu* ~ 0.6, where Eu* is the value of Eu interpolated between Sm and Gd). The $^{87}Sr/^{86}Sr$ ratios show a wide range with initial values from 0.7072 to 0.7123. These values are comparable to those found in rocks of similar composition and age from the Eastern Alps (Del Moro et al. 1981, and unpublished; Borsi et al. 1978, 1979).

Ultrapotassic lamprophyres (UK). These resemble the orenditic rocks of the Betic Cordillera, Spain (Fuster et al. 1967; Lopez-Ruiz and Rodriguez Badiola 1980; Venturelli et al., in press) and the minette of Sisco, Corsica (Velde 1967), and exhibit the following geochemical features: low Al_2O_3, low to moderate V, high K/Na ratio and high P_2O_5, Zr, Hf, Rb, K, light-REE contents, unusually high Th (average 155 ppm) and U (average 33 ppm), strongly fractionated REE patterns ($Ce_N/Yb_N = 32$–40, where N indicates chondrite normalized values; Fig. 4) and moderate Nb, low Nb/Y and high Zr/Nb ratios, high MgO, Ni and Cr values. The $^{87}Sr/^{86}Sr$ ratios are higher than those of the coeval andesite dykes and intrusive rocks, and cover a wide range of values (initial ratios = 0.7165–0.7216). Moreover, the high-K Alpine lamprophyres as well as ultrapotassic rocks from other orogenic areas, differ from the ultrapotassic rocks occurring in the cratonic areas (Africa, Western Australia) in having, for instance, higher P_2O_5/TiO_2 ratios (> 0.3) and in showing negative 'anomalies' of Nb, Ta, Ti in MORB-normalized diagrams (cf Pearce et al. 1981). Within each of the groups of rocks studied, the high and variable $^{87}Sr/^{86}Sr$ ratios do not show good correlations with other parameters such as SiO_2, Rb/Sr and Sr(or 1/Sr) (Fig. 5). However, the SG and UK rocks have progressively higher Sr contents, Rb/Sr ratios (reflecting the high Rb contents), and $^{87}Sr/^{86}Sr$ in comparison with the CG rocks.

Petrogenesis

Shallow-level fractional crystallization

The trace element and strontium isotope data indicate that shallow level fractional crystallization cannot account for

Table 3. Representative chemical analyses of calc-alkaline (CG), shoshonitic (SG) and ultrapotassic (UK) rocks from the Western Alps

	CG								SH			UK					
	Basalt	Basaltic andesites					Andesites		Basalt	Latites							
	118	695	1729	214	1710	1433	319	251	96	1064	241	216	242	243b	1698	1627	247
SiO_2	48.6	53.0	53.1	53.3	54.0	54.0	59.2	59.3	49.4	59.1	60.0	60.4	49.3	50.2	54.8	56.0	56.0
TiO_2	0.97	1.61	1.10	0.99	1.10	0.60	0.69	0.63	0.93	0.69	0.53	0.54	1.05	1.06	1.50	1.4	1.24
Al_2O_3	16.1	17.4	17.2	17.1	15.2	14.3	16.5	17.5	13.4	16.5	17.3	17.4	11.3	10.8	8.87	8.9	11.0
Fe_2O_3	3.72	1.35	1.33	2.07	1.33	1.98	2.25	1.64	1.51	5.69	2.14	2.06	1.63	1.81	2.05	2.0	2.21
FeO	5.15	8.49	6.68	5.10	5.76	5.25	3.45	3.48	5.96	0.60	3.39	3.12	4.60	5.23	3.76	3.3	2.65
MnO	0.17	0.18	0.16	0.15	0.17	0.15	0.09	0.11	0.16	0.09	0.10	0.11	0.10	0.11	0.18	0.11	0.09
MgO	6.53	4.32	4.96	5.32	6.66	7.52	4.04	2.85	10.9	1.88	2.10	2.04	13.6	12.9	9.54	9.4	9.27
CaO	12.4	8.27	6.83	7.31	8.00	8.91	5.22	5.08	8.32	4.23	3.76	4.34	7.65	6.43	4.33	4.2	4.11
Na_2O	2.42	2.13	2.46	2.68	2.27	2.05	3.23	3.27	1.95	3.31	3.37	3.59	1.60	0.85	1.78	1.9	1.29
K_2O	0.93	1.37	2.65	2.54	2.37	1.43	2.85	2.89	2.87	4.91	4.38	4.09	5.94	6.72	9.40	9.6	9.07
P_2O_5	0.67	0.26	0.27	0.39	0.47	0.26	0.19	0.18	0.70	0.53	0.37	0.37	1.10	1.19	1.40	1.2	1.09
L.O.I.	2.6	1.6	3.1	3.2	3.0	3.3	2.3	2.9	3.5	2.8	2.3	2.1	2.3	2.5	2.0	1.6	1.8
Total	100.3	100.0	99.8	100.2	100.2	99.8	100.0	99.8	99.6	100.3	99.7	100.2	100.2	99.8	99.6	99.6	99.8

$(^{87}Sr/^{86}Sr)_t \pm \sigma$		*0.7074* *±4*	*0.7113* *±2*	*0.7125* *±2*		*0.7087* *±2*	*0.7076* *±4*	*0.7117* *±2*	*0.7126* *±3*	*0.7120* *±2*	*0.7124* *±2*	*0.7112* *±2*	*0.7171* *±3*	*0.7179* *±1*		*0.7221* *±2*	*0.7178* *±4*
$(^{87}Sr/^{86}Sr)_o$		0.7072	0.7111	0.7122		0.7086	0.7075	0.7115	0.7123	0.7117	0.7119	0.7108	0.7166	0.7172		0.7216	0.7165
V	255	315	205	140	190	215	148	100	160	125	80	85	125	125	80	110	95
Cr	124	(30)	77	161	350	417	(40)	<30	590	(35)	(31)	<30	802	839	660	586	600
Ni	43	(20)	25	72	92	100	(10)	29	333	(30)	(10)	(20)	395	460	364	315	396
Cu	7	16	9	15	91	68	26	(4)	53	55	(4)	–	9	72	36	10	46
Zn	87	90	102	123	67	68	81	79	90	65	68	59	83	116	115	87	84
Li	10	29	19	29	13	18	15	19	23	22	23	14	32	33	23	20	42
Rb	–	48	90	106	–	47	83	87	140	261	210	189	321	388	–	443	569
Sr	–	320	521	540	–	475	1120	682	580	988	543	597	809	688	–	1242	544
Y	25	(50)	31	32	26	20	25	26	32	43	37	40	36	46	68	55	47
Zr	128	124	120	175	125	106	198	151	236	358	364	356	375	450	854	730	592
Nb	10	(11)	11	13	15	8	–	10	17	37	27	22	26	28	54	40	50
Hf	3.09	2.99	3.18	–	3.06	2.38	(3.4)	–	–	9.59	8.87	8.58	10.6	11.9	–	21.6	16.1
Ta	0.53	0.70	0.53	–	0.68	0.40	1.27	–	–	2.42	2.43	2.71	1.61	1.65	–	2.08	2.33
Th	16.2	–	6.19	–	16.3	11.1	20.1	–	–	146	137	135	122	136	–	226	140
U	4.5	–	2.5	–	4.2	2.9	12.0	–	–	31	34.2	34.5	–	–	–	33	–
La	30.4	–	22.7	–	25.2	21.9	51.3	–	–	–	80.2	80.7	–	–	–	164	–
Ce	60.2	32.1	44.1	–	50.7	41.6	93.4	–	–	150	151	152	213	265	–	357	258
Nd	33.4	22.2	24.3	–	30.9	22.6	42.5	–	–	80.3	63.9	64.5	140	173	–	227	175
Sm	6.7	–	5.2	–	6.4	4.5	7.2	–	–	–	11.1	11.0	–	–	–	–	–
Eu	1.79	1.73	1.43	–	1.40	1.11	1.58	–	–	2.45	1.91	1.93	4.71	5.28	–	7.65	5.33
Gd	(8.4)	7.1	5.7	–	–	(6.0)	(8.3)	–	–	–	–	–	–	–	–	–	–
Tb	0.82	1.14	0.81	–	0.73	0.61	0.73	–	–	1.20	1.26	1.27	1.79	2.04	–	2.91	1.95
Tm	(0.39)	0.78	0.52	–	0.38	0.38	0.36	–	–	0.46	0.48	0.47	(0.37)	(0.41)	–	–	(0.37)
Yb	2.17	4.14	2.50	–	1.93	1.84	1.92	–	–	2.42	2.82	2.84	1.70	1.81	–	2.34	1.70
Lu	0.26	0.50	0.36	–	(0.23)	0.22	(0.19)	–	–	–	–	–	–	–	–	–	–
Ce/Yb	28	7.8	18	–	26	23	49	–	–	62	54	54	125	146	–	153	153
Zr/Y	5.1	2.5	3.9	5.5	4.8	5.3	7.9	5.8	7.4	8.3	9.8	8.9	10	9.8	12.5	13	12.5
Rb/Sr	–	0.15	0.17	0.20	–	0.10	0.07	0.13	0.24	0.26	0.39	0.32	0.31	0.56	–	0.36	1.05
K/Rb	–	237	244	199	–	253	285	276	170	156	173	180	154	144	–	180	132

( ), less accurate data; $(^{87}Sr/^{86}Sr)_t$. actual isotope ratio: $(^{87}Sr/^{86}Sr)_o$. Isotope ratio at 31 m.y. before present. The Y data are referred to Y = 44 ppm for BCR-1

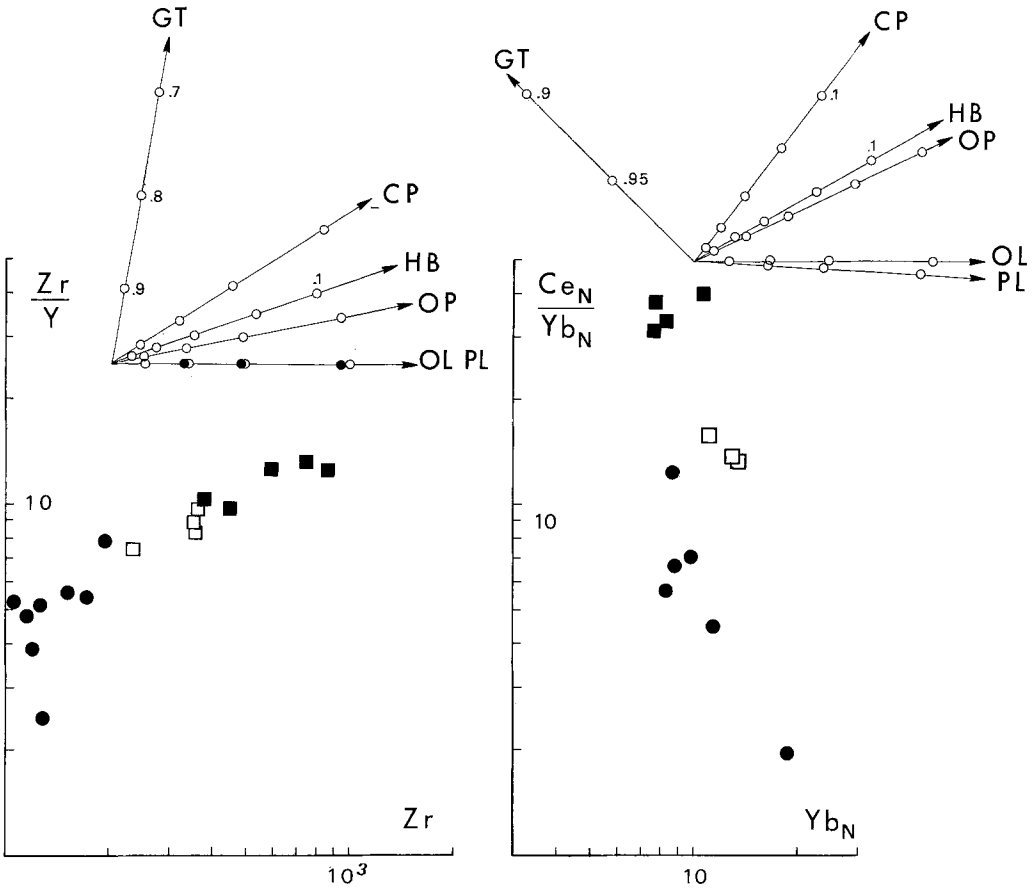

Fig. 6. (a) Plots of Zr/Y against Zr, and (b) Ce_N/Yb_N against Yb_N. Symbols as in Fig. 2. At the top, the vectors indicate the fractional crystallization paths for the indicated minerals; *GT*, garnet; *CP*, clinopyroxene, *HB*, hornblende, *OP*, orthopyroxene, *OL*, olivine and *PL*, plagioclase. Partition coefficients are from Pearce and Norry (1979) for Zr and Y, and Arth (1976) for Ce and Yb. The circles and dots along the vectors indicate the fraction of residual melt, ie. 0.8, 0.6, 0.4, 0.2 proceeding from the origin of the vector

the variations within or between the volcanic groups. The plots of Zr/Y against Y and Ce_N/Yb_N against Yb_N (Fig. 6) show that variations are inconsistent with fractional crystallization involving olivine ± plagioclase ± pyroxene ± amphibole. Although the negative Eu anomalies in the latites (e.g. $Eu/Eu^* = 0.6$ in samples 216 and 241) are consistent with plagioclase fractionation, the proportion of crystallization required (assuming $FO_2 = 10^{-8}$; Fudali 1965; Drory and Ulmer 1974) is very high and is inconsistent with the trace element data noted above. Finally, the variations of initial $^{87}Sr/^{86}Sr$ ratio both within and between the CG, SH and UK groups (Table 3) precludes any simple petrogenetic scheme based on shallow-level fractional crystallization.

Fractional crystallization at intermediate and high pressures (over ca. 10 kbar)

The low Yb concentration (below 10 times chondrite) in the investigated rocks and the negative correlation of Ce_N/Yb_N and Yb_N for the calcalkaline samples (Fig. 6) suggest that garnet may have been present in the phases fractionated from the magmas or in the source. Fractional crystallization of garnet is consistent with the occasional occurrence of garnet phenocrysts in some late Alpine magmatic rocks (Boegel 1975, and references therein) but there is no direct evidence of garnet crystallization in the investigated rocks. However, the varied Sr isotope ratios preclude simple models based on fractional crystallization at shallow and/or great depths, and indicate that the magmas are derived from a heterogeneous source. The role of source composition and partial melting processes are therefore investigated below.

Partial melting and source composition

The analyzed rocks have high Ce/Ta (52–172), Th/Nb (0.6–6.1) and Th/Ta (12–109) ratios similar to those of lavas from active margins (Ce/Ta over 60, Th/Nb over 0.2 and Th/Ta over 3.5; cf. Bailey 1981; Pearce 1982). Therefore, although there is a high concentration of elements generally enriched in 'within plate' lavas (e.g. LREE, Zr), there is evidence for the influence of subduction processes. For example, the negative Nb, Ta and Ti 'anomalies' (Fig. 7), which also characterize the most magnesian rocks may reflect (i) stability of Fe–Ti-oxides at high P_{H_2O} (cf Hellmann and Green 1979) during the partial melting of the source or in the subducted material during dehydration/partial melting as well as (ii) early separation of Fe–Ti-oxides. The last interpretation is less plausible for the investigated rocks since the negative anomalies also occur in the ultrapotassic rocks, where Cr-spinel rather than Fe–Ti-oxide is the early crystallizing phase. The relatively high and variable $^{87}Sr/^{86}Sr$ ratio (0.7072–0.7216) suggests involvement of crustal material.

For the calc-alkaline basalt/basaltic andesites, the relatively high MgO, Ni (Fig. 8) and Cr, and the coexistence with mantle-derived rocks (see below) are consistent with derivation from upper mantle material. In this case, the

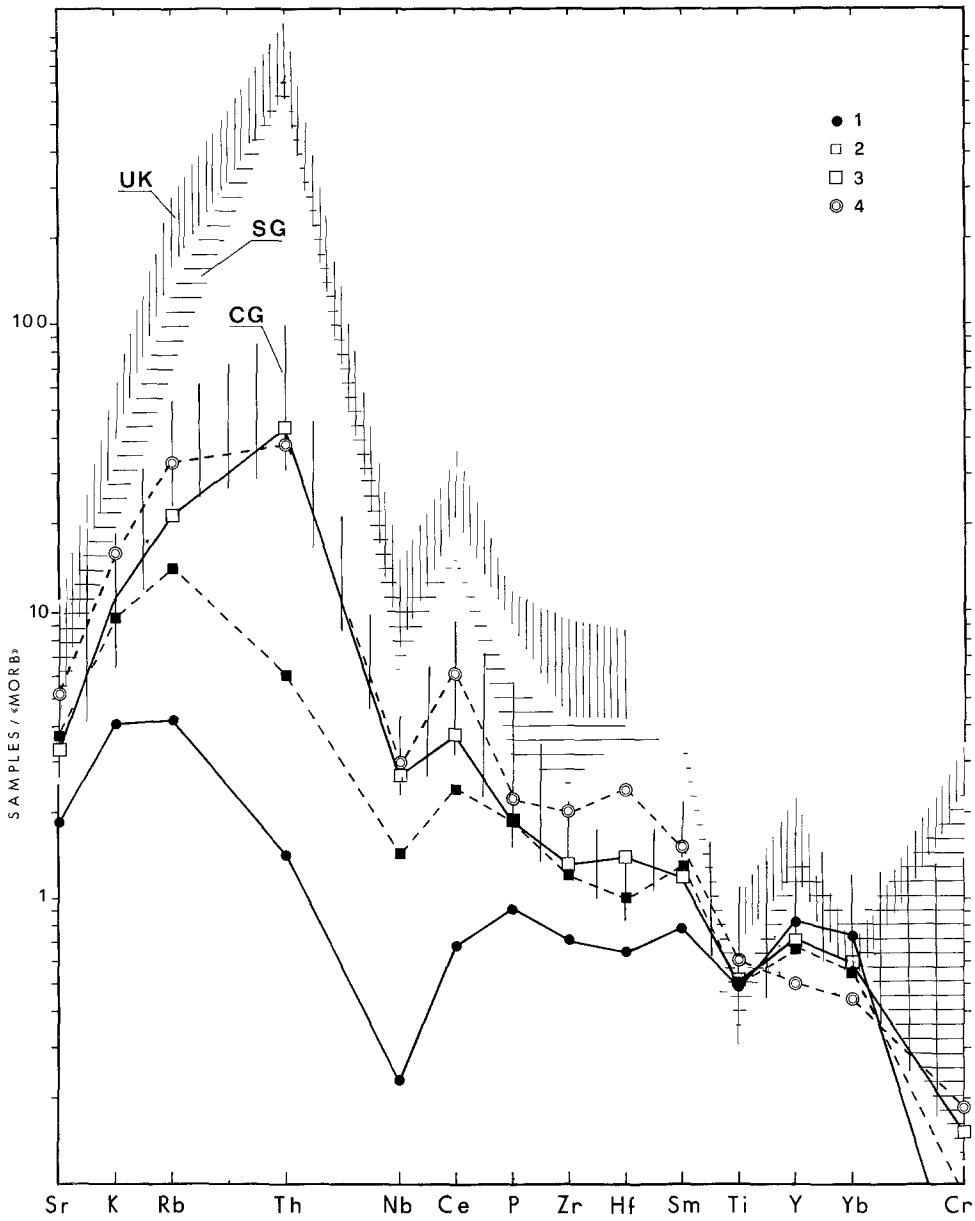

Fig. 7. Normalized trace element patterns for the analysed and other orogenic rocks. The normalizing values (average MORB) are from Pearce et al. (1981). UK, SG, CG indicate the fields for ultrapotassic, shoshonitic and calc-alkaline rocks from the Western Alps. The other patterns refer to average values compiled by Bailey (1981): 1, low-K andesites of oceanic island arcs; 2, other andesites from oceanic island arcs; 3, continental island arcs; 4, active continental margins with thick crust

varied REE patterns (Fig. 4) and the range of initial $^{87}Sr/^{86}Sr$ (0.7072–0.7115; Table 2) may reflect crustal assimilation into one or more mantle-derived magmas (cf. De Paolo 1981). A similar model may be applied to the shoshonitic basalt (sample 96).

The ultrapotassic lamprophyres pose the most interesting petrogenetic problems. The high Ni, Cr, MgO contents and the unusually high *mg*-number (0.79–0.83) of these rocks are consistent with an origin by partial melting of ultramafic mantle material. The predicted *mg*-number for mantle olivine is about 0.92–0.94 (Roeder and Emslie 1970); such high values represent the uppermost values of the Mg/(Mg+Fe+Mn) ratio in olivine of ultramafic assemblages. The Ni/Mg ratio in the analyzed lamprophyres (Ni ppm/MgO% = 29–43) is higher than that of other rocks with comparable SiO_2 and with high to moderate Ni contents (Fig. 8). This may reflect the effect of increasing H_2O and alkaline element contents (mainly K) and of increasing pressure on decreasing the value of D_{Ol}^{Ni}, or an important contribution of mantle phlogopite (incongruent melting) characterized by a high Ni/MgO ratio (cf. Venturelli et al., in press).

The ultrapotassic rocks have Rb/Sr and $^{87}Sr/^{86}Sr$ ratio values unusually high for mantle products (cf. Hawkesworth 1982). It has been recently proposed by McCulloch et al. (1983) that some Australian lamproites may be derived from ancient (>1000 Ma) enriched mantle with very high $^{87}Sr/^{86}Sr$ ratios. However, the persistence of a mantle unmodified for a long time below the Alpine orogenic belt seems unlikely in view of the complex history of the area.

Assuming that the volcanic rocks may be derived by partial melting of mantle peridotite, Table 4 shows the re-

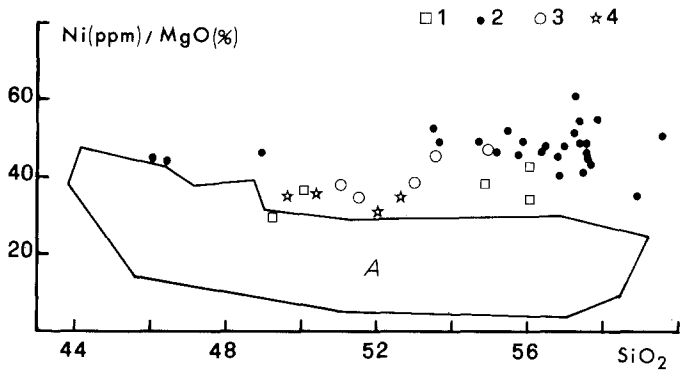

Fig. 8. Plot of Ni (ppm)/MgO (%) against SiO_2 for orenditic rocks from several localities: 1, K-rich lamprophyres from the Western Alps; 2, K-rich rocks from SE Spain (Venturelli et al. in press); 3, wyomingites and orendites from the Leucite Hills (Kuehner et al. 1981); 4, -rich dykes from Antarctica (Sheraton and England 1980). Field A includes samples with intermediate to high Ni contents belonging to several tectonic settings (e.g. komatiites, high-Mg andesites/boninites, low-Ti ophiolites; data available from G. Venturelli). All the samples used for the diagram have MgO in the range 6.5–20%

sults of calculations of expected element ratios in melts derived by partial melting of peridotite with the composition of 'primordial mantle' of Wood (1979). The element ratios and melt fractions have been calculated assuming that the Zr content of the sample reflects the degree of partial (batch) melting. The results in Table 4 indicate that the Rb/K, Rb/Zr, K/Zr and Ce/Zr ratios are much higher than expected by varied degrees of partial melting of 'primordial mantle'. Further, the degrees of partial melting, between 9–10% for the CG rocks to 1–3% for the UK rocks, is unrealistically low. This implies that the Zr content of the rocks may be considered to be higher than expected from mantle partial melting. The enrichment factors (C_s/C_c, where C_s is the element concentration in the sample and C_c the estimated concentration) decrease in the order $E_{Th} > > E_{Rb} > E_K > E_{Ce}$ and increase proceeding from the calc-alkaline to the ultrapotassic rocks. The Rb/K ratio increases from the calc-alkaline to the ultrapotassic rocks (Table 4). Since Rb and K are not significantly fractionated during partial melting of a "normal" mantle (olivine + orthopyroxene + clinopyroxene ± spinel ± garnet) the variation of the Rb/K ratio suggests the presence, in the source, of phases able to fractionate these elements (e.g. phlogopite) which contributed in different amounts to the melt.

It is concluded that the mantle source of the magmas investigated required additional components enriched in incompatible elements. Considering the geological history of the Alpine region from the Cretaceous, varied mantle metasomatism (vapour phase/silicate melt) under high P_{H_2O} and P_{O_2} conditions is likely to have accompanied the subduction processes. An important contribution of phlogopite to the ultrapotassic melts is consistent with the low Na_2O contents and the relatively high K_2O/Na_2O ratios of these rocks. However, taking into account the high contents of Sr (544–1242 ppm) in the ultrapotassic rocks, it is unlikely that the high $^{87}Sr/^{86}Sr$ ratios are due only to the contribution from highly radiogenic mica, which has a low total Sr content but also from Sr-rich mineral phases within the source with higher Sr-isotope ratios. The trace element (and hence Sr isotope) enrichment of the source may be interpreted in terms of processes occurring during subduction of oceanic crust between the African and Eurasian plates. During this subduction, some parts of the Pennine and Austroalpine continental crust experienced high pressure metamorphism (eclogite-glaucophane facies; cf. Section 2), and it is likely that Hercynian and pre-Hercynian granitoids and paragneiss and continent-derived oceanic sediments may have been subducted (Hunziker 1974). Dehydration and melting of these materials may then have been responsible for the trace element and Sr isotope enrichment of the mantle source of the volcanic rocks. As an alternative hypothesis, the ultrapotassic rocks may be derived from superheated mantle magmas strongly contaminated by highly radiogenic continental crust material. However, the high K_2O/Na_2O ratio and the low Na_2O content of the investigated rocks are inconsistent with this interpretation.

The origin of the rocks of intermediate composition is more ambiguous. These rocks show large variations in Sr-isotope ratios (0.7075–0.7119) which are similar to upper crustal values. The most simple process to explain the genesis of these rocks is fractional crystallization at shallow depth of several magmas with different geochemical and isotopic characteristics associated with assimilation of crustal material.

The high thermal gradient under the Alpine chain at the time of the magma genesis, as suggested by the Lepontine metamorphism (cf. Section 2), as well as proposed thermal models for the Alps (e.g. England 1978) suggests the

Table 4. Ranges of actual and calculated element ratios for some investigated rocks (samples 118, 1710, 1433, 96, 242, 243b, 1677, 247)

	$Rb/K \times 10^{-3}$	Rb/Zr	$Th/Zr \times 10^{-2}$	K/Zr	Ce/Zr	F
CG	3.95	0.4	10–13	60–157	0.39–0.47	0.085–0.10
SG	5.9	0.6	nd	101	nd	0.045
UK	5.6–7.6	0.6–0.9	24–33	91–132	0.44–0.59	0.013–0.03
calculated	3.5	0.08–0.09	0.87–0.89	21–23	0.12–0.16	
D_{bulk}		Rb	Th	K	Ce	Zr
$Ol_{70}Opx_{25}Cpx_5$		0.00023	0.00035	0.00048	0.0075	0.0102
$Ol_{60}Opx_{25}Cpx_{10}Gt_5$		0.00040	0.00097	0.00153	0.0119	0.0299

The element ratios and the melt fractions (F) have been calculated considering the Zr content in the samples as reflecting different degrees of partial melting (batch melting) of 'primordial mantle' (Wood 1979) and using the partition coefficients (D_{bulk}) and residual mantle mineralogy listed obove

possibility of partial melting of the lower crust, or of basaltic eclogites which may represent remnants of subducted oceanic crust. The REE distribution in the investigated rocks is consistent with this hypothesis. According to the calculations performed by Apted (1981), the intermediate rocks investigated may have been derived by a relatively low degree (ca. 15–20%) of modal melting of eclogite (ca. Gt 40% Cpx 60%) with ca. 25 (for the calc-alkaline andesites) to 35 times (for the latites) chondritic concentrations of HREE and Ce_N/Tm_N = ca. 1.4. These characteristics are consistent with the REE distribution in the metabasalts and eclogites of the Alpine and Apennine belt (Venturelli et al. 1981; Ernst et al. 1983) which, before metamorphism, constituted a portion of the oceanic crust likely to have been involved in the subduction processes during the Cretaceous.

Summary

The post ophiolitic magmatic history of the Alpine chain is complex and may be summarized as follows.

1-Evidence of Cretaceous-Palaeocene (?) magmatic activity related to subduction is lacking or scarcely documented along the Alpine belt. By contrast, Tertiary magmatic products of orogenic affinity are widespread along the Alps close to the Insubric Lineament, from the Aosta valley to the Austria-Jugoslavia boundary. The geological evolution of the Alpine chain suggests that this magmatic activity was not directly related to active subduction of oceanic crust, but to thermal relaxation subsequent to the collision between the European and African plates. The Lepontine metamorphism (thermal peak at ca. 38 Ma), which developed under compressional conditions, was the first result of the thermal updoming. The Oligocene magmatism represents a further geological event under similar thermal conditions but related to tensional tectonics. The volcanic rocks may be classified as calc-alkaline, shoshonitic and ultrapotassic in character.

2-The overall correlation of Rb/Sr with $^{87}Sr/^{86}Sr$ proceeding from the calc-alkaline to the ultrapotassic rocks is consistent with a varied contribution of low Rb/Sr and $^{87}Sr/^{86}Sr$ mantle material and of crustal components characterized by higher $^{87}Sr/^{86}Sr$ and Rb/Sr ratios. The crustal component (oceanic + continental crust) was probably added to the mantle mainly by extensive metasomatism during the Eoalpine subduction which accompanied the closure of the Tethyan ocean in the investigated area, and by interaction between the uprising magmas and the continental crust. The ultrapotassic rocks may have been derived from parental magmas generated by partial melting of mantle material which experienced extensive metasomatism processes involving addition of incompatible trace elements and radiogenic continental crust components. It is noteworthy that the Alpine ultrapotassic rocks occur only within the area where there is direct evidence of subduction involving the continental crust (the eclogitic micaschists of the Sesia-Lanzo Zone).

3-The parent melts of the calc-alkaline and shoshonitic rocks may have generated by variable degrees of partial melting of less enriched mantle. However, the origin of the intermediate rocks is ambiguous. In addition to the possibility of fractional crystallization from several parental magmas, they may have been also produced by partial melting of oceanic or of deep continental crust material or by mixing of mantle melts and lower continental crust material close to the Moho. The analytical data do not allow us to choose among these different hypotheses.

Acknowledgements. The authors are grateful to Dr. J.C. Hunziker, who collaborated with one of us on the problems of the Alpine magmatism, and to Dr. J. Dostal and Prof. S. Capedri for the valuable suggestions. Drs. O. Williams Thorpe, S. Tonarini, G. Pardini and U. Giannotti and Mr. J. Watson are thanked for their assistance during INAA analysis and Rb-Sr determinations. The University of London Reactor Centre, Ascot are gratefully acknowledged for irradiation facilities. The research has been supported by CNR, Rome, ct 80.00945.05 and by Ministero della Pubblica Istruzione, Rome, 1981 (responsible Prof. F. Giammetti).

References

Apted MJ (1981) Rare Earth elements systematics of hydrous liquids from partial melting of basaltic eclogite: a re-evaluation. Earth Planet Sci Lett 52:172–182

Arth JG (1976) Behaviour of trace elements during magmatic processes – a summary of theoretical models and their applications. J Res US Geol Surv 4:41–47

Bailey JC (1981) Geochemical criteria for a refined discrimination of orogenic andesites. Chem Geol 32:139–154

Barton M, Hamilton DL (1982) Water-undersaturated melting experiments bearing upon the origin of potassium-rich magmas. Mineral Mag 45:267–278

Beccaluva L, Gatto GO, Gregnanin A, Piccirillo E (1979) Geochemistry and petrology of dyke magmatism in the Alto Adige (Eastern Alps) and its geodynamic implications. Neues Jahrb Geol Paleontol Monatsh 6:331–339

Boegel J (1975) Zur Literatur über die 'Periadriatische Naht'. Verh Geol B-A Wien 1975 (2–3):163–199

Bocquet J, Delaloye M, Hunziker JC, Krummenacher D (1974) K-Ar and Rb-Sr dating on blue amphiboles, micas and associated minerals from the Western Alps. Contrib Mineral Petrol 47:7–26

Borsi S, Del Moro A, Sassi FP, Zirpoli G (1978) On the age of the periadriatic Rensen massif (Eastern Alps). Neues Jahrb Geol Paleontol Monatsh 5:267–275

Borsi S, Del Moro A, Sassi FP, Zirpolo G (1979) On the age of the Vedrette di Ries (Rieserferner) massif and its geodynamic significance. Geol Rundsch 68:41–60

Carraro F, Ferrara G (1968) Alpine 'tonalite' at Miagliano, Biella (zona Diorite-Kinzigitica). Schweiz Mineral Petrogr Mitt 48:75–80

Dal Piaz GV, Ernst WG (1978) Areal geology and petrology of eclogites and associated metabasites of the Piemonte Ophiolite Nappe, Breuil-St-Jacques area, Italian Western Alps. Tectonophysics 51:99–126

Dal Piaz GV, Hunziker JC, Martinotti G (1972) La Zona Sesia-Lanzo e l'evoluzione tectonico-metamorfica delle Alpi nordoccidentali interne. Mem Soc Geol Ital 11:433–466

Dal Piaz GV, Hunziker JC, Martinotti G (1973) Excursion to the Sesia Zone of the Schw Mineral-Petrograph Gesellschaft, September 30th to October 3rd, 1973. Schweiz Mineral Petrogr Mitt:447–490

Dal Piaz G, Hunziker JC, Stern WB (1978) The Sesia-Lanzo Zone, a slice of subducted continental crust. Geol Surv Open-File Rep 78–701:83–86

Dal Piaz GV, Venturelli G, Scolari A (1979) Calc-alkaline to ultrapotassic postcollisional volcanic activity in the Internal Northwestern Alps. Mem Soc Geol 32:1–16

Delaloye M, Sawatzki G (1975) Géochronométrie de élément volcaniques du flysch helvétique du synclinal de Thone (Haute Savoie, France). Archives Soc Genève 28:95–99

Del Moro A, Dal Piaz GV, Martin S, Venturelli G (1981) Dati radiometrici e geochimici preliminari su magmatiti oligoceniche del settore meridionale del massiccio Ortles-Cevedale. Rend Soc Geol Ital 4:265–266

De Marco L (1959) Su alcuni filoni lamprofirici radioattivi del

complesso Sesia-Lanzo. Studi Ricerche Div Geomin CNEN 1:1–30
De Paolo JD (1981) Trace element and isotopic effects of combined wallrock assimilation and fractional crystallization. Earth Planet Sci Lett 53:189–202
Drory A, Ulmer GC (1974) Oxygen fugacity determination for Cascadian andesites. EOS 55:487
England PC (1978) Some thermal considerations of the Alpine metamorphism-past, present and future. Tectonophysics 46:21–40
Ernst WG, Rambaldi E, Piccardo GB (1983) Trace element geochemistry of iron and titanium-rich eclogitic rocks, Gruppo di Voltri, Western Liguria. J Geol 91:413–425
Frey M, Hunziker JC, Frank W, Bocquet J, Dal Piaz GV, Jäger E, Niggli E (1974) Alpine metamorphism of the Alps: a review. Schweiz Mineral Petrogr Mitt 54:247–290
Fudali RF (1965) Oxygen fugacities of basaltic and andesitic magmas. Geochim Cosmochim Acta 29:1063–1075
Fuster JM, Gastesi P, Sagredo J, Fermoso ML (1967) Las rocas lamproiticas del SE de Espana. Estudios Geol 23:35–69
Gosso G, Dal Piaz GV, Piovano V, Polino R (1979) High pressure emplacement of early-Alpine nappes, postnappe deformations and structural levels (Internal Northwestern Alps) Mem Soc Geol 32:1–15
Hawkesworth CJ (1982) Isotope characteristics of magmas erupted along destructive plate margins. In: Thorpe RS (ed) Andesites: Orogenic andesites and related rocks, Wiley and Sons, New York 1982, pp 549–571
Hellman PL, Green TH (1979) The role of sphene as an accessory phase in the high pressure partial melting of hydrous compositions. Earth Planet Sci Lett 42:191–201
Hunziker JC, (1974) Rb-Sr age determination and the Alpine tectonic history of the Western Alps. Mem Ist Geol Min Univ Padova 31:1–54
Jäger E (1973) Die Alpine Orogenese im Lichte der radiometrischen Alterbestimmung. Eclogeo Geol Helv 66:11–21
Krummenacher D, Evernden JF (1960) Détermination d'age isotopique faites sur quelques roches des Alpes par le méthode potassium-argon. Schweiz Mineral Petrogr Mitt 40:267–277
Kuehner SM, Edgar AD, Arima M (1981) Petrogenesis of the ultrapotassic rocks from the Leucite Hills, Wyoming. Am Mineral 66:663–677
Laubscher HP (1969) Mountain building, Tectonophysics 7:551–563
Laubscher HP (1974) Evoluzione e struttura delle Alpi. Le Scienze: 72:48–59
Lopez Ruiz J, Rodriguez Badiola E (1980) La region volcanica del sudeste de Espana. Estud Geol 36:5–63
Martini J (1968) Etude petrographique des gres de Taveyanne entre Arve e Giffre (Haute Savoie, France). Schweiz Mineral Petrogr Mitt 48:539–564
McCulloch MT, Jaques AL, Nelson DR, Lewis JD (1983) Nd and Sr isotopes in kimberlites and lamproites from Western Australia: an enriched mantle origin. Nature 302:400–403
Nakamura N (1974) Determination of REE, Ba, Fe, My, Na and K in carbonaceous chondrites. Geochim Cosmochim Acta 38:757–775
Niggli E (1973) Metamorphic map of Europe. UNESCO, Paris, 1973
Pearce JA (1982) Trace element characteristics of lavas from destructive plate boundaries. In: Thorpe RS (ed) Andesites: Orogenic andesites and related rocks, Wiley and Sons, New York: 525–548
Pearce JA, Alabaster A, Shelton AW, Searle MP (1981) The Oman ophiolite as a Cretaceous arc-basin complex: evidence and implications. Phil Trans R Soc Lond A300:299–317
Pearce JA, Norry MJ (1979) Petrogenetic implications of Ti, Zr, Y and Nb variations in volcanic rocks. Contrib Mineral Petrol 69:33–47
Peccerillo A, Taylor SR (1976) Geochemistry of Eocene calcalkaline rocks from the Kastaniony area, Northern Turkey. Contrib Mineral Petrol 58:63–81
Potts PJ, Thorpe OW, Watson JS (1981) Determination of rare-earth element abundances in 29 international rock standards by instrumental neutron activation analysis: a critical appraisal of calibration errors. Chem Geol 34:331–352
Roeder PL, Emslie RF (1970) Olivine-liquid equilibrium. Contrib Mineral Petrol 29:275–289
Scheuring B, Ahrendt H, Hunziker JC, Zingg A (1974) Paleobotanical and geochronological evidence for the Alpine age of the metamorphism in the Sesia Zone. Geol Rundsch 63:305–326
Sheraton JW, England RN (1980) Highly potassic dykes from Antarctica. J Geol Soc Aus 27:129–135
Velde D (1967) Sur un lamprophyre hyperalcalin potassique: la minette de Sisco (ile de Corse). Bull Soc Mineral Crist France 90:214–223
Venturelli G, Capedri S, Di Battistini G, Crawford A, Kogarko LN, Celestini S. The ultrapotassic rocks from SE Spain. Lithos (in press)
Venturelli G, Thorpe RS, Potts PJ (1981) Rare earth and trace element characteristics of ophiolitic metabasalts from the Alpine-Apennine belt. Earth Planet Sci Lett 53:109–113
Wagner GA, Reimer GM, Jager E (1977) Cooling ages derived by apatite fission track, mica RB-Sr and K-Ar dating; the uplift and cooling history of the central Alps. Mem Ist Geol Mineral Univ Padova 30:1–27
Wood DA (1979) A variably veined suboceanic upper mantle-Genetic significance for mid-ocean ridge basalts from geochemical evidence. Geology 7:499–503
Zingg A, Hunziker JC, Frey M, Ahrendt H (1976) Age and degree of metamorphism of the Canavese Zone and the sedimentary cover of the Sesia Zone. Schweiz Mineral Petrogr Mitt 56:361–375

Received June 10, 1983; Accepted March 2, 1984